



# Journal of Applied Sciences

ISSN 1812-5654

**science**  
alert

**ANSI***net*  
an open access publisher  
<http://ansinet.com>

## Lightning Electromagnetic Fields Modeling Using an Indirect Hybrid Method- Interaction with an Overhead Power Line

<sup>1</sup>Zin Eddine Azzouz, Boualem Ghemri, <sup>2</sup>Abdenbi Mimouni and <sup>3</sup>Abderrezzak Cherifi

<sup>1</sup>Laboratoire de Modélisation des Systèmes Electrotechniques et Systèmes Experts-U.S.T.O. «Mb»  
B.P. 1505 El M'Naouar, Oran 31000, Algeria

<sup>2</sup>Laboratoire de Réseaux Electriques, Ecole Polytechnique Fédérale de Lausanne,  
EPFL STI LRE, ELL 036, Station 11, CH 1015 Lausanne, Suisse

<sup>3</sup>Laboratoire d'Ingénierie des Systèmes de Versailles, 45 Avenue des Etats Unis 78000, Versailles, France

---

**Abstract:** This contribution deals with the computation of lightning return stroke electromagnetic fields and overvoltages induced by coupling between these fields and an overhead power line. For the first objective use is made of a hybrid technique based on a lightning current distribution model typically the MTLE model. The hybrid technique is based partially on FDTD method for the calculation of electric field components after magnetic flux density evaluation using the images theory. The computational results are compared with experimental measurements taken from literature. The second part of this paper is devoted to the investigation of interaction between lightning electromagnetic fields and an overhead line. For this purpose a computer program was developed by authors based on a time domain coupling model. The simulation results are validated by experimental ones obtained using a reduced scale line model illuminated by the EMP simulator of the Swiss Federal Institute of Technology in Lausanne.

**Key words:** Electromagnetic compatibility (EMC), lightning electromagnetic fields, modeling, finite time domain (FDTD), lightning induced overvoltages

---

### INTRODUCTION

Lightning electromagnetic pulse (LEMP) effects assume a special concern in the modern society. Besides the safety aspects regarding the danger to people and damages to classified areas, the necessity to predict the radiated lightning electromagnetic pulses (LEMP) has been increasing since high susceptibility equipment has been used in almost all domains of activities (Sartori and Cardoso, 2000). Indeed, lightning is a major natural source of electromagnetic radiation that interferes with modern electronic and communication systems and can damage a wide range of electrical/electronically systems. Accurate knowledge of LEMP distribution at a given location is essential in determining the threat level for a sensitive system, for achieving an efficient isolation design of electric power networks and for determining electromagnetic compatibility requirements of telecommunication systems (Yang and Zhou, 2004; Baba *et al.*, 2004).

For the calculation of electromagnetic fields generated by subsequent lightning return strokes, several methods have been performed by different research

groups around the world (Yang and Zhou, 2004; Rakov, 2001; Rachidi, 1991; Shoory *et al.*, 2003; Uman and McLain, 1971; Rubinstein and Uman, 1989). Among these methods we distinguish the Finite Difference Time Domain (FDTD) method which is a simple and efficient tool for the treatment of electromagnetic environment of complex structures directly struck by lightning or indirectly affected by the radiated lightning electromagnetic fields (Tirkas *et al.*, 1993). However there are some difficulties related to this technique. One of these difficulties reside in the analysis of low-frequency transients, in which the space-discretization step is several hundreds or thousands times smaller than the minimum wavelength associated to the maximum frequency excited by the source. It's the case of the analysis relative to lightning interaction with complex structures commonly found in reality. Thus, in order to take in account this difficulty in the lightning electromagnetic fields calculations we propose the application of an alternative procedure namely the hybrid method based partially on FDTD method for the electric field component computation and the temporal method for the magnetic field component evaluation. The latest

consists of integrating infinitesimal current dipoles through the channel length using the images theory. This procedure is particularly motivated by the fact that there is a general agreement in the specialised literature for the magnetic field results. In return, this literature shows quite different results concerning the intensity and wave shape of the near electric field (Sartori and Cardoso, 2000; Nucci *et al.*, 1993).

The hybrid method was successfully tested by Sartori and Cardoso (2000) and validated with theoretical results published in (Rubinstein and Uman, 1991). Thus, Sartori *et al.* (2000) have considered, for the calculating of the magnetic flux density, the spatial-temporal distribution of the current in each radiating dipole as a step function. In the framework of this paper, our contribution in the use of this method deals with the calculation of the magnetic flux density employing engineering models especially: the MTLE model, introduced by Nucci *et al.* (1993) for the representation of the lightning channel current distribution since it is reported to give a reasonable agreement with measurements. Moreover this modeling is motivated by Rakov and Uman (1998) which have ranked the MTLE model among the best engineering models with regard to entirety of the testing results and mathematical simplicity.

Once the lightning electromagnetic fields calculated, they are used as an input to electromagnetic coupling models to compute the induced voltages or currents on overhead lines. These lightning overvoltages are nowadays a major issue in Electro Magnetic Compatibility (EMC) and power quality domains. Indeed, the need for a good quality in power supply along with the widespread use of sensitive devices connected to distribution lines makes the protection against lightning induced disturbances of primary importance. Moreover, the establishment of a good protection schemes of overhead power lines against lightning-induced overvoltages, necessity a good understanding of the mechanism by which lightning-generated electromagnetic fields interact with these lines.

**MODELING AND CALCULATION OF LIGHTNING ELECTROMAGNETIC FIELDS**

**A. Geometry of the problem:** Figure 1 shows a schematic representation of the lightning channel’s assumed geometry and indicates the observation point P where the magnetic flux density is calculated. Generally, the calculation of the electric and magnetic fields associated with cloud-to-ground lightning return stroke is based on certain number of commonly-adopted assumptions (Uman and Mclain, 1971; Rubinstein and Uman, 1989), namely:

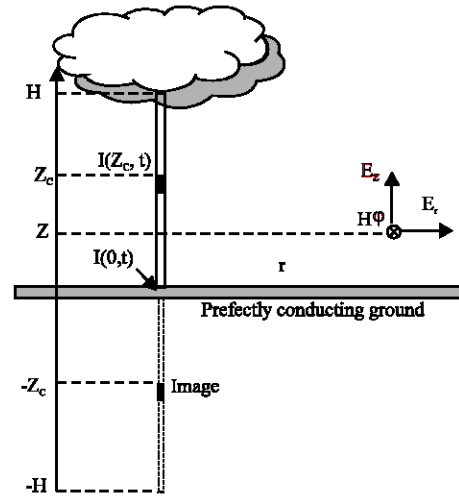


Fig. 1: Lightning channel geometry

- The lightning channel is represented by a straight vertical antenna along which the return stroke front propagates upward at the return stroke speed;
- The ground is assumed flat, homogenous and characterized by its conductivity and its relative permittivity.

**B. Formulation of the hybrid method**

**Magnetic field calculation:** The magnetic field component at the location  $P(r, \phi, z)$  produced by a short vertical section of infinitesimal channel  $dz'$  at height  $z'$  carrying a time-varying current  $i(z', t)$  can be computed in the time domain using the following relation:

$$H_\phi(x, y, z, t) = \frac{1}{4\pi\mu_0} \int_{-H}^H \left[ \left( \frac{r}{R^3} i(z_c, t - R/c) + \left( \frac{r}{cR^2} \frac{\partial i}{\partial t} (z_c, \tau - R/c) \right) dz \right) \right] \quad (1)$$

With

$$R = \sqrt{(x^2 + y^2)^2 + (z - z_c)^2} \quad (2)$$

Where,  $i(z', t)$  is the current carried by the  $dz'$  dipole at time  $t$ ;  $\mu_0$  the vacuum permeability,  $c$  the speed of light in vacuum,  $R$  the distance from the dipole to the observation point and  $r$  the horizontal distance between the channel and the observation point.

In the literature several return stroke models are used in the LEMP calculations. In this paper the MTLE (Modified Transmission Line-exponential) model was adopted (Rakov, 2001; Nucci *et al.*, 1993) for the lightning current distribution. The current intensity is supposed to decay exponentially while propagating up the channel as expressed by:

$$z_c < v.t \ i(z_c,t) = e^{-z\lambda} \cdot i(0, t- z_c/v) \tag{3}$$

$$z_c > v.t \ i(z_c,t) = 0 \tag{4}$$

$$z_c > H \ i(z_c,t) = 0 \tag{5}$$

Where the  $\lambda$  factor is the decay constant and  $v$  is the speed of propagating of the return stroke.

For the representation of the channel-base current  $i_0(t)$ , a sum of two functions has been chosen in order to better reproduce the overall wave shape of the current as observed in typical experimental results. We have chosen the current parameters reported in Table 1 and 2 in order to reproduce the typical features of the lightning current at the channel base-namely the peak value, maximum time derivative and decay time-of a typical subsequent return stroke, in accordance with observations of Nucci *et al.* (1993) and Heidler (1985):

$$I(0, t) = i_1(t) + i_2(t) \tag{6}$$

$$i_1(t) = \frac{I_1}{\eta_1} \cdot \left[ \frac{(t/\tau_{11})^{n_1}}{1 + (t/\tau_{11})} \right] \cdot \exp(t/\tau_{12}) \tag{7}$$

$$i_2(t) = \frac{I_2}{\eta_2} \cdot \left[ \frac{(t/\tau_{21})^{n_2}}{1 + (t/\tau_{21})} \right] \cdot \exp(t/\tau_{22}) \tag{8}$$

$$\eta_1 = \exp[(\tau_{11}/\tau_{12}) \cdot (n_1 \cdot \tau_{11} / \tau_{12})^{1/n_1}] \tag{9}$$

Where:

$I_1(1,2)$  is the amplitude of  $i_1(i_2)$ ,  $\tau_{11}(\tau_{21})$  the front time constant of  $i_1(i_2)$ ,  $\tau_{12}(\tau_{22})$  the decay time constant of  $i_1(i_2)$ ,  $\eta_{1,2}$  the amplitude correction factor and  $n_{1,2}$  is an exponent having values between 2 to 10.

**Electric field calculation:** The electric field computation is performed using the FDTD method. It is based on the direct solution of the difference form of Maxwell's equations by means of the Yee discretization scheme. The technique has the advantage of being very flexible and it is easy to implement it in a computer code (Sarto, 2001).

In this procedure the electric field is numerically evaluated by a simplified FDTD approach applied to the basic Maxwell equation given in (10):

$$\nabla \times \vec{B} = \mu(\vec{J} + \frac{\partial \vec{D}}{\partial t}) = \mu(\sigma \vec{E} + \epsilon \frac{\partial \vec{E}}{\partial t}) \tag{10}$$

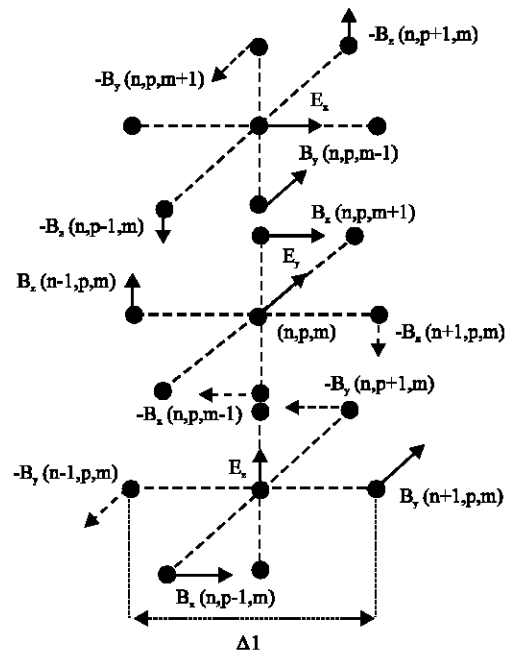


Fig. 2: Positions of the field components

Where,  $\mu$  is the permeability;  $\sigma$  is the conductivity;  $\epsilon$  is the permittivity;  $\vec{j}$  is the current density vector and  $\vec{J}$  is the electric flux density vector.

The vector Eq. 10 represents a system of three scalar equations, which can be expressed in a rectangular coordinate system through their (x, y, z) components as:

$$\frac{\partial E_z}{\partial t} = \frac{1}{\mu\epsilon} \left( \frac{\partial B_y}{\partial x} - \frac{\partial B_x}{\partial y} - \mu\sigma E_z \right) \tag{11}$$

$$\frac{\partial E_x}{\partial t} = \frac{1}{\mu\epsilon} \left( \frac{\partial B_z}{\partial y} - \frac{\partial B_y}{\partial z} - \mu\sigma E_x \right) \tag{12}$$

$$\frac{\partial E_y}{\partial t} = \frac{1}{\mu\epsilon} \left( \frac{\partial B_x}{\partial z} - \frac{\partial B_z}{\partial x} - \mu\sigma E_y \right) \tag{13}$$

The FDTD method is applied in the solution of Eq. 11-13. This calculating method consists of a space and time approximation derivatives by central finite differences scheme (Fig. 2) (Sadiku, 1992). This approximation can be written as,

$$\frac{\partial F(n, p, m, k)}{\partial z} = \frac{F(n, p, m + 1, k) - F(n, p, m - 1, k)}{\Delta l} \tag{14}$$

$$\frac{\partial F(n, p, m, k)}{\partial t} = \frac{F(n, p, m, k + 1/2) - F(n, p, m, k - 1/2)}{\Delta t} \tag{15}$$

The notation  $F(n, p, m, k)$  is the grid point of the space, the variable  $\Delta l$  is the length between two series nodes and  $\Delta t$  the propagation time (assumed to be the time step related to the magnetic flux density values).

We can rewrite Eq. 11-13 with applying Eq. 14-15. The electric field components  $E_x$ ,  $E_y$  and  $E_z$  can be calculated as:

$$E_x(n,p,m,k+1/2)=E_x(n,p,m,k-1/2)+\frac{c^2\Delta t}{\Delta l} [B_x(n,p+1,m,k)-B_x(n,p-1,m,k)+B_y(n,p,m-1,k)-B_y(n,p,m+1,k)] \quad (16)$$

$$E_y(n,p,m,k+1/2)=E_y(n,p,m,k-1/2)+\frac{c^2\Delta t}{\Delta l} [B_x(n,p,m+1,k)-B_x(n,p,m-1,k)+B_z(n-1,p,m,k)-B_z(n+1,p,m,k)] \quad (17)$$

$$E_z(n,p,m,k+1/2)=E_z(n,p,m,k-1/2)+\frac{c^2\Delta t}{\Delta l} [B_y(n+1,p,m,k)-B_y(n-1,p,m,k)+B_x(n,p-1,m,k)-B_x(n,p+1,m,k)] \quad (18)$$

**Procedure implementation:** The procedure consists in first of evaluating the magnetic flux density, by integrating the Eq. 1, at six points around the point where the electric field will be calculated. The electric field is computed with the approach described below in Eq. 16-18. The FDTD algorithm requires specific considerations. Thus the grid size  $\Delta l$  should be a fraction of wavelength. In addition, to avoid a numerical instability, the time increment should be bounded by the grid size values. The typical choice is referred to this equation:

$$\Delta t \leq \Delta l / 2c \quad (19)$$

Finally, this procedure has the particularity that the electromagnetic field can be evaluated without meshing the entire of the configuration. It is an important feature which can be translated in term of memory space reducing.

**RESULTS**

In step with the lightning channel base and the lightning channel currents parameters two cases have been considered for presentation of the results. The lightning channel base current parameters corresponding to the case 1 are reported in Table 1. For this case the lightning channel current parameters are:  $\lambda = 2 \text{ km}$  and  $v = 1.5 \cdot 10^8 \text{ m sec}^{-1}$ .

For the case 2, the lightning channel base current parameters are registered in Table 2 and Fig. 3. The lightning channel current parameters are in this case:  $\lambda = 1.5 \text{ km}$  and  $v = 1 \cdot 10^8 \text{ m sec}^{-1}$ .

Table 1: Lightning channel base current parameters

$I_1$	$\tau_{11}$	$\tau_{12}$	$n_1$	$I_2$	$\tau_{21}$	$\tau_{22}$	$n_2$
10.5 kA	2 $\mu\text{s}$	4.8 $\mu\text{s}$	2	9 kA	20 $\mu\text{s}$	26 $\mu\text{s}$	2

Table 2: Lightning channel base current parameters

$I_1$	$\tau_{11}$	$\tau_{12}$	$n_1$	$I_2$	$\tau_{21}$	$\tau_{22}$	$n_2$
19.5 kA	1 $\mu\text{s}$	2 $\mu\text{s}$	2	12 kA	8 $\mu\text{s}$	30 $\mu\text{s}$	2

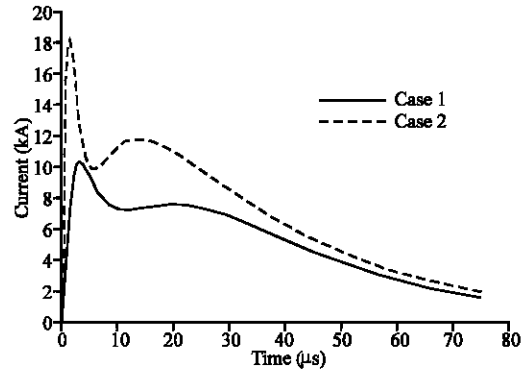


Fig. 3: Lightning channel base current wave shapes according to the parameters of Table 1 and 2

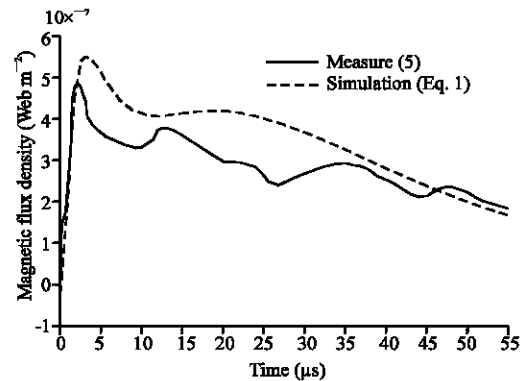


Fig. 4: Comparison between the calculated magnetic flux densities and the measured fields (case 1)

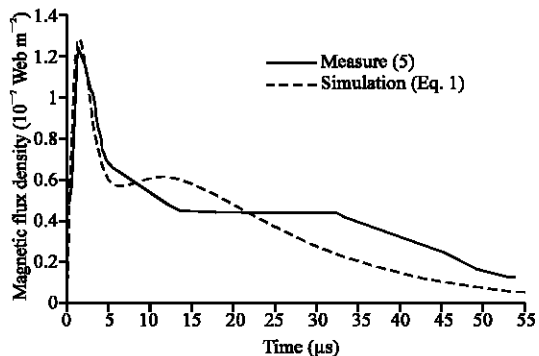


Fig. 5: Comparison between the calculated magnetic flux densities and the measured fields (case 2)

In Fig. 4 and 5 the magnetic field density wave shapes obtained by integration of Eq. 1 and corresponding to case 1 and 2, are presented. In the same

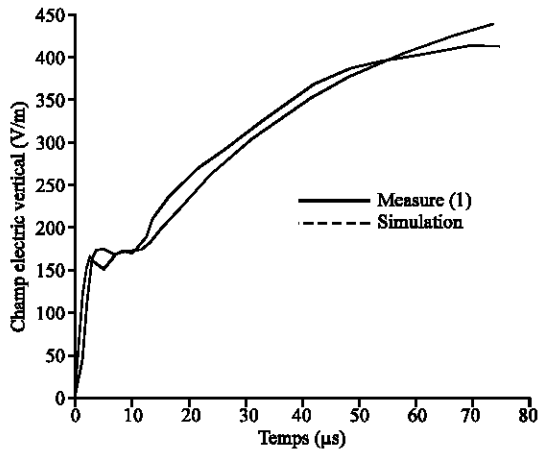


Fig. 6: Comparison between the calculated vertical electric and the measured field at 2Km from the striking point (case 1)

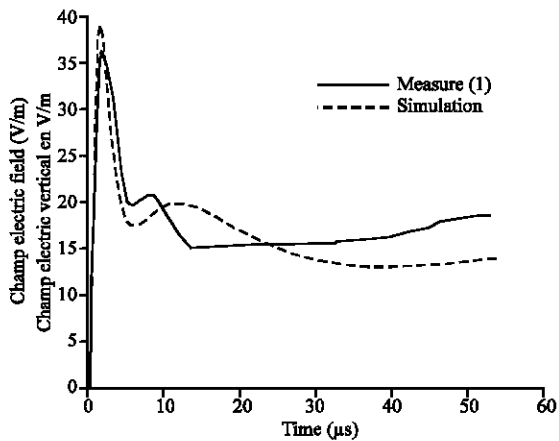


Fig. 7: Comparison between the calculated vertical electric and the measured field at 9 km from the striking point (case 2)

figures, experimental measures of the same field taken from (Rachidi, 1991) are also plotted. It is easy to show the satisfactory agreement, between the calculated values and the measured one.

Plots of the calculated vertical electric field at 2 km from the striking point and of the measured one (Rachidi, 1991) are found in Fig. 6. These results have been obtained for the lightning channel base and the lightning channel currents parameters corresponding to case 1. In Fig. 7 we present the theoretical and measured variations of the vertical electric field at 9 km relative to the lightning channel base and the lightning channel currents parameters of case 2. It can be seen from these figures the good agreement between the simulation and the measured results.

In these figures, the dashed line is the experimental curve published in (Rachidi, 1991) and the full line the theoretical curve obtained by the hybrid method.

Finally we can say that a good agreement exist between the results regarding the wave shapes of the vertical electric field and some differences in the peak values reaching about ten percent in the worst case are observed. The hybrid approach and the program developed by authors are then validated.

### INTERACTION BETWEEN THE CALCULATED ELECTROMAGNETIC FIELD AND AN ELECTRICAL LINE

The two coupling models most frequently used in the power lightning literature for the calculation of lightning induced overvoltages are namely the Chowdhuri and Gross model and the Agrawal, Price and Gurbaxani model. These two models are compared and discussed in (Nucci *et al.*, 1995); it was showed that the Chowdhuri-Gross model is incomplete. Only the Agrawal model and its equivalent formulations can be considered as rigorous within the limits of the adopted hypothesis (transmission line approximations) (Nucci and Rachidi, 1999).

Lightning ElectroMagnetic Pulse LEMP to transmission line coupling equation can be dealt with either in the frequency domain or in the time domain. A time domain approach allows handling in more straightforward way non-linearities which appear when considering corona effect and/or when protective devices such as surge arresters are present. One of the popular approaches to solve the transmission line coupling equations in time domain is the Finite Difference Time Domain (FDTD) technique.

**Coupling model:** The Agrawal and *al* coupling model is used for calculating the induced voltages on a overhead line following an external electromagnetic field aggression. The basic assumptions are:

- The overhead line can be treated as lossless.
- The electric field is assumed to propagate unaffected by the ground.
- The Modified Transmission Line (MTL) model is used for the lightning channel.
- The overhead line is matched with its characteristic impedance.

Starting from Maxwell's equations and adopting the transmission line assumption, it is possible to derive a pair of equations describing the coupling of an external electromagnetic field and a single conductor line. These

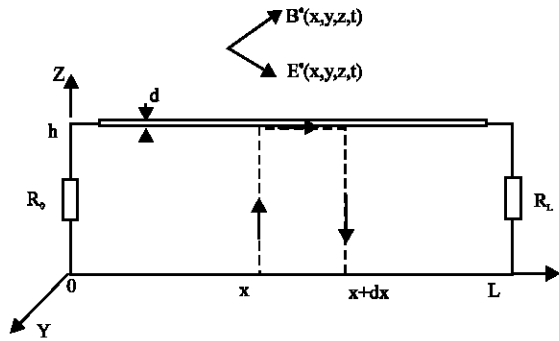


Fig. 8: Geometry of the line under study illuminated by a non-uniform electromagnetic field

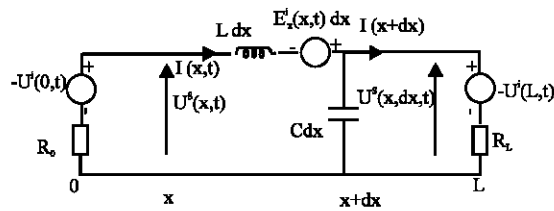


Fig. 9: Differential equivalent coupling circuit according to the Agrawal and al. for a lossless single wire overhead line

equations can be written in different equivalent formulations. The formulation of Agrawal and al. for the case of a lossless line, is given by (Fig. 8):

$$\frac{\partial v^s(x,t)}{\partial x} + L \frac{\partial i(x,t)}{\partial t} = E_x^e(x,h,t) \quad (20)$$

$$\frac{\partial i(x,t)}{\partial x} + C \frac{\partial v^s(x,t)}{\partial t} = j(x,t) \quad (21)$$

Where  $E_x^e(x,h,t)$  is the horizontal component of the incident electric field along the x axis at the conductor's height h;  $j(x,t)$  the current source, L the inductance per unit length of the line, C the capacitance per unit length of the line,  $i(x,t)$  the induced current and  $v^s(x,t)$  the scattered voltage related to  $v(x,t)$  by the following expression:

$$v(x,t) = v^s(x,t) + v^i(x,t) \quad (22)$$

$$v^i(x,t) = -\int_0^h E_z^e(x,z,t) dz \quad (23)$$

Where  $E_z^e(x,z,t)$  is the exciting (or inducing) vertical electric field that can be considered as unvarying in the height range  $0 < z < h$  and  $v^i(x,t)$  the incident voltage.

The equivalent coupling circuit according to the Agrawal model is shown in Fig. 9.

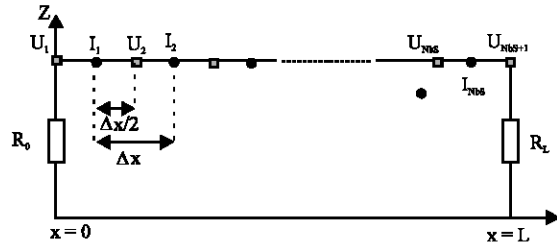


Fig. 10: Schematic representation of the spatial discretization along the line

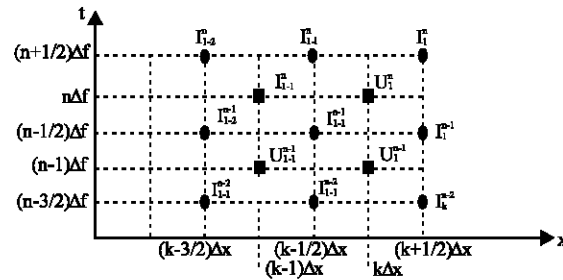


Fig. 11: Time and spatial discretization

**Point-Centered Finite Difference Time Domain Technique (FDTD):** First, we proceed to make a schematic representation of the spatial discretization of the line (Fig. 10).

The current and the exciting horizontal electric field are calculated at the same points. The voltages are calculated at the medium points between two points of current. Therefore the current and the voltage are shifted by a half spatial step.

For the temporal discretization, the current is bringing forward of half temporal step with regard to the voltage, (Fig. 11). The temporal and the spatial steps must check the following stability condition:

$$\Delta t \cdot v_p < \Delta x \quad (24)$$

Where:

$$v_p = \sqrt{\frac{1}{LC}} \quad (25)$$

If  $\Delta t \cdot v_p = \Delta x$ , the FDTD method give the best solution.

The scattered voltage, calculated at the voltage nodes and at the instant  $n \cdot \Delta t$  is given by:

$$U_k^n = v^s((k-1)\Delta x, n\Delta t), 0 \leq k \leq K_{max} + 1 \quad (26)$$

The current, calculated at the current nodes and at the instant  $(n+0.5\Delta t)$ :

$$I_k^n = I((k-0.5)\Delta x, (n+0.5)\Delta t), 1 \leq k \leq K_{max} \quad (27)$$

The horizontal electric field, calculated at the current nodes and at the instant  $n\Delta t$ :

$$E_k^n = E_x((k - 0.5)\Delta x, n\Delta t), 1 \leq k \leq K_{max} \quad (28)$$

The current sources, calculated at the voltage nodes and at the instant  $(n-0.5)\Delta t$ , are null at all nodes of voltage, except at the two extremities of the line, they are expressed as:

$$j_k^n = j((k - 1)\Delta x, (n - 0.5)\Delta t), 1 \leq k \leq K_{max} + 1 \quad (29)$$

The two vertical electric fields, calculated at the two extremities of the line are:

$$E_{z1}^n = E_z(0, (n - 0.5)\Delta t) \quad (30)$$

$$E_{z2}^n = E_z(N_{max}\Delta x, (n - 0.5)\Delta t) \quad (31)$$

First coupling equation:

$$\frac{\partial v^s(x, t)}{\partial x} + L \frac{\partial i(x, t)}{\partial t} = E_x^e(x, h, t) \quad (32)$$

At the point  $((k-0.5)\Delta x, n\Delta t)$  we can write:

$$\frac{\partial v^s(x, t)}{\partial x} = \frac{U_{k+1}^n + U_k^n}{\Delta x} \quad (33)$$

$$\frac{\partial i(x, t)}{\partial t} = \frac{I_k^n + I_k^{n-1}}{\Delta t} \quad (34)$$

$$E_x^e(x, h, t) = E_k^n \quad (35)$$

After several developments we obtain:

$$I_k^n = \frac{\Delta t}{L} (E_k^n - \frac{U_{k+1}^n - U_k^n}{\Delta x} + \frac{L}{\Delta t} I_k^{n-1}), 1 \leq k \leq K_{max} \quad (36)$$

Second coupling equation:

$$\frac{\partial i(x, t)}{\partial x} + C \frac{\partial v^s(x, t)}{\partial t} = j(x, t) \quad (37)$$

At the point  $((k-1)\Delta x, (n-0.5)\Delta t)$  we can write:

$$\frac{\partial i(x, t)}{\partial x} = \frac{I_k^{n-1} - I_{k-1}^{n-1}}{\Delta x} \quad (38)$$

$$\frac{\partial v^s(x, t)}{\partial t} = \frac{U_k^n - U_k^{n-1}}{\Delta t} \quad (39)$$

$$j(x, t) = j_k^n \quad (40)$$

For  $2 \leq k \leq K_{max}$  the scattered voltage is:

$$U_k^n = \frac{\Delta t}{C} (-\frac{I_k^{n-1} - I_{k-1}^{n-1}}{\Delta x} + \frac{C}{\Delta t} U_k^{n-1}) \quad (41)$$

For  $k = 1$  and  $k = k_{max}$  and for resistive terminations, the following boundary conditions are introduced:

$$U_0^n = -R_0 I_0^n + \int_0^h E_{z1}^n dz \quad (42)$$

$$U_{k_{max}}^n = -R_L I_{k_{max}}^n + \int_0^h E_{z2}^n dz \quad (43)$$

Two fictive current nodes are introduced at 0 and  $k_{max}+1$ . The voltage sources created by the vertical electric fields  $E_{z1}$  and  $E_{z2}$  are transformed to current sources and the capacitance per unit length of the line  $C$  is replaced by  $C/2$ . Thus we obtained the following expressions:

$$j(0, (n - 0.5)\Delta t) = j_1^n = \frac{hE_{z1}^n}{R_0} \quad (44)$$

$$j(L, (n - 0.5)\Delta t) = j_{k_{max}+1}^n = \frac{hE_{z2}^n}{R_L} \quad (45)$$

Finally we obtain:

$$U_1^n = (\frac{C}{2\Delta t} + \frac{1}{2R_0\Delta x})^{-1} (\frac{hE_{z1}^n}{R_0\Delta x} - \frac{I_1^{n-1}}{\Delta x} + (\frac{C}{2\Delta t} - \frac{1}{2R_0\Delta x})U_1^{n-1}) \quad (46)$$

$$U_{k_{max}+1}^n = (\frac{C}{2\Delta t} + \frac{1}{2R_L\Delta x})^{-1} (\frac{hE_{z2}^n}{R_L\Delta x} + \frac{I_{k_{max}}^{n-1}}{\Delta x} + (\frac{C}{2\Delta t} - \frac{1}{2R_L\Delta x})U_{k_{max}+1}^{n-1}) \quad (47)$$

**Experimental validation of the coupling program:** The simulation result namely the induced current in a line are obtained using a program developed by authors based on the Agrawal coupling model. In the purpose of the validation of this simulation result by an experimental test, we have considered as an input of the





Fig. 12: SEMIRAMIS EMP simulator

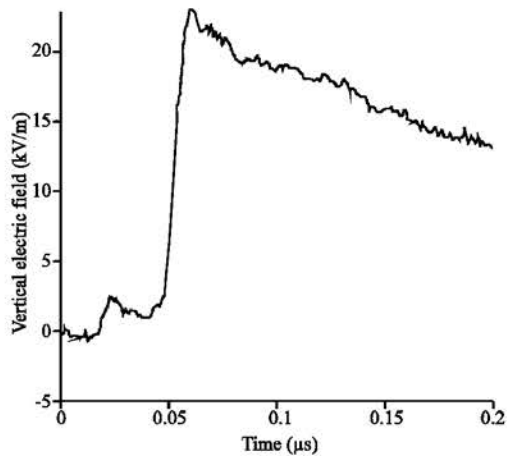


Fig. 13: Vertical electric field inside its working volume in absence of the line

coupling program, the experimentally vertical electric field given in (Paolone *et al.*, 2004) consisting of a bounded wave vertically-polarized type with a working volume of  $3 \times 1 \times 1$  m (Fig. 12). The waveform of this electric vertical field inside the working volume, performed in absence of the line, is presented in Fig. 13.

The experimentally test is performed using a reduced scale line model illuminated by the EMP simulator of the Swiss Federal Institute of Technology in Lausanne (SEMIRAMIS, for a detailed description of the simulator, (Arreghini *et al.*, 1993).

Line parameters:

Height  $h = 20$  cm,

Length  $l = 2$  m.

Diameter:  $d = 1.4$  mm,

Terminal resistances:  $R_0 = 680 \Omega$  and  $R_L = 680 \Omega$ .

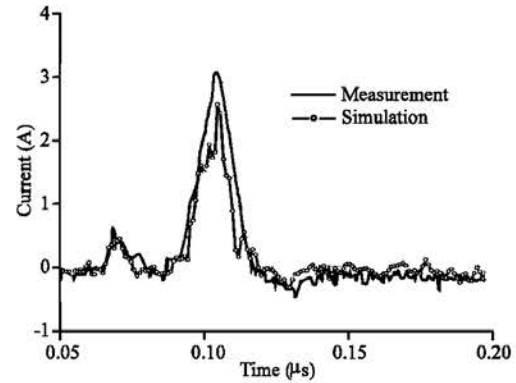


Fig. 14: Induced current on the overhead line: Computed current predicted by the Agrawal model. Measured current adopted from (Paolone *et al.*, 2004).

Simulation parameters:

$$\Delta t = 1 \text{ ns}, \Delta x = 0.4 \text{ cm}, t_{\text{max}} = 0.2 \mu\text{s}$$

Line inductance per unit length:

$$L = (\mu_0 / (2 * \pi)) * \ln(4 * h / d);$$

Line capacitance per unit length:

$$C = \mu_0 * \epsilon_0 / L$$

Figure 14 shows a comparison between the predicted waveform of the induced current, obtained using our program based on the Agrawal coupling model and the experimental vertical electric field and the measured one. It can be seen that our simulation allows us to obtain a good approximation of the experimental waveform.

**Induced voltages computation using the calculated electromagnetic fields:** The geometrical configuration under study is composed of a single wire transmission line (Fig. 15). The latest is matched with its characteristic impedance and has a length  $l$  of 1000 m and a height  $h$  of 10 m.

The striking point is considered to be symmetrical with regard of the two extremities of the line and is situated at a distance of 50 m (Fig. 16). The assumption of a perfectly conductor ground was adopted for the electromagnetic field calculation because the more remote point is at a distance of 500 m. Moreover, the line resistance and the cross conductance have been neglected.

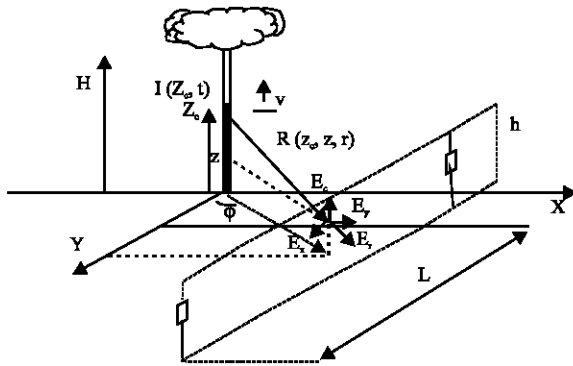


Fig. 15: Geometry of the line under study

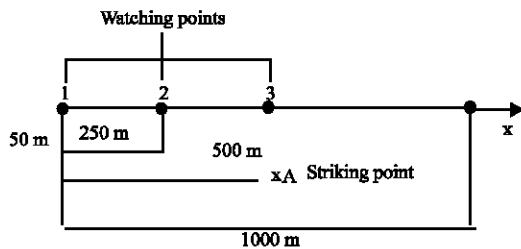


Fig. 16: Position of the striking point

Table 3: Lightning channel base current parameters

$I_1$ (kA)	$\tau_{11}$ ( $\mu$ s)	$\tau_{12}$ ( $\mu$ s)	$n_1$	$I_2$ (kA)	$\tau_{21}$ ( $\mu$ s)	$\tau_{22}$ ( $\mu$ s)	$n_2$
10.5	0.25	2.5	2	6.5	2.1	230	2

The electromagnetic field was calculated using the hybrid method and the MTL model of the current distribution in the lightning channel. The attenuation parameter  $\lambda$  has been assumed as 2 km and the velocity of electromagnetic wave  $v$  as  $1.5 \cdot 10^8$  m sec<sup>-1</sup>. The lightning channel base current parameters used in this study are given in Table 3.

**Induced voltages computation in different points of the line:** In Fig. 17 the temporal induced overvoltages variations corresponding to the three calculating points considered (namely at the extremities  $x_1 = -500$  m; at 250 m from the extremities; at the middle of the line  $x_3 = 0$  m) are drawn together. From these results it is easy to see that the total overvoltage along the line is a positive unipolar wave for all the considered points in the line. Each overvoltage waveform is characterised by short and very steep rise times. In the other hand the maximum of voltage appear at the observation point very close to the lightning channel.

**Temporal variations of the induced overvoltage in step with the striking point distance:** In this study three different striking point distances have been considered namely:  $d_1 = 25$  m,  $d_2 = 50$  m and  $d_3 = 100$  m. For each

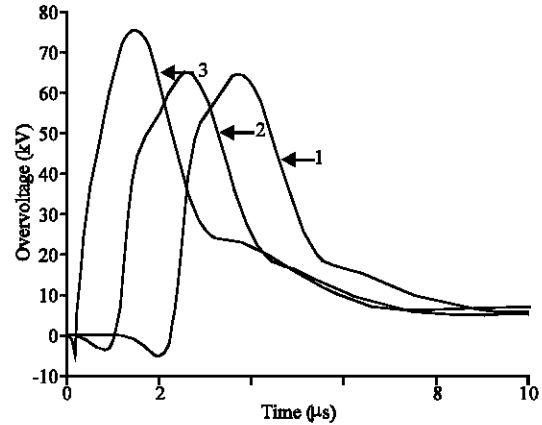


Fig. 17: Induced overvoltages calculated in different points of the line

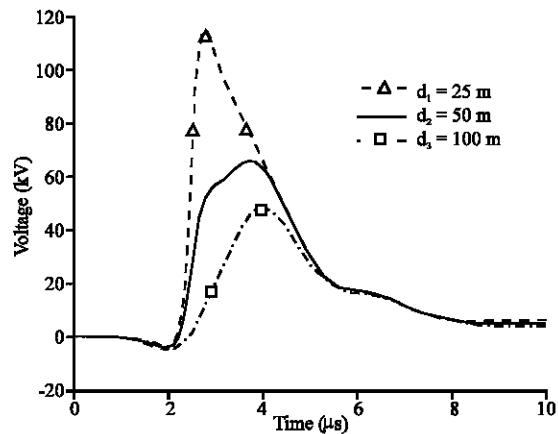


Fig. 18: Temporal variations of the induced overvoltage in step with the striking point distance

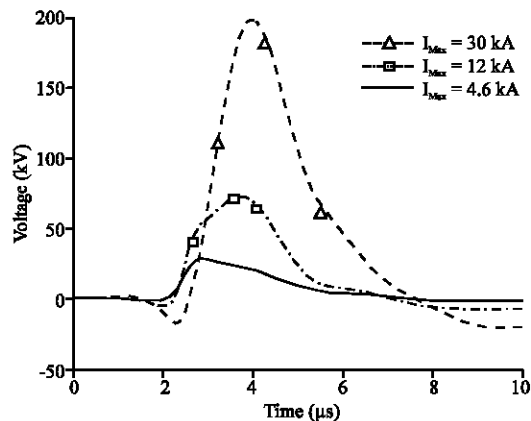


Fig. 19: Influence of the lightning channel base current peak value on the induced overvoltage

distance we have calculated the corresponding overvoltages. The waveforms of these overvoltages are plotted in Fig. 18. This result shows that the induced

overvoltage is important as we get closer to the striking point. This allows another validation of the computer program developed by authors and the adopted coupling model.

**Influence of the lightning channel base current peak value on the induced overvoltages:** The study has consisted on varying the lightning channel base current peak value and the calculating at each variation the amplitude of the induced overvoltage. The obtained results are presented in Fig. 19. Thus we can see from this figure that the induced overvoltage amplitude increases proportionally with the lightning channel base current peak value increasing. Hence the influence is typically linear.

### CONCLUSIONS

A presentation of a numerical approach for predicting the lightning electromagnetic field referred to a return stroke model has been described in this paper in fact the hybrid technique. The numerical results obtained by this approach have been validated by comparative studies with experiments measures. It is shown that the hybrid approach leads to a good agreement results comparatively with the experimental measures for the case of perfect ground conductivity. Otherwise, the numerical implementation of the hybrid method represents a good alternative in the studies of LEMP interaction with complex electrical structures because it is very adapted to such structures. The second part of this paper was devoted to the investigation of lightning electromagnetic fields interaction with an overhead line. The computation results hence the coupling program developed by authors were validated by experimental results obtained using a reduced scale line model illuminated by the EMP simulator of the Swiss Federal Institute of Technology in Lausanne (SEMIRAMIS).

There is a good agreement in the first few microseconds. The disagreement is due to the simulation parameters employed to solving the two coupling equations (the choice of spatial and temporal step, the line parameters...). But, the comparison confirms the validity of the Agrawal model.

We have also shown that a coupling model can describe the electromagnetic field coupling to transmission lines in terms of different components of the electromagnetic field.

As perspective, we suggest the introduction of the lossy ground effects, the effect of periodically grounded shielding wire and surge arresters on the lightning induced voltages.

### ACKNOWLEDGEMENTS

The authors wish to thank the staff of the laboratory LRE of the Swiss Federal Institute of Technology in Lausanne, in particular Dr. Farhad Rachidi and Dr. Pierre Zweiacker for their helpful, by giving them the values of the electric field and the results of the current of the experimental test SEMIRAMIS.

### REFERENCES

- Arreghini, F., M. Ianoz, P. Zweiacker, D.V. Giri and A. Tehori, 1993. SEMIRAMIS: An asymmetrical bounded wave EMP simulator with a good confinement inside the transmission line. In Proceeding of the 10th International Symposium on Electromagnetic Compatibility, Zurich, Switzerland, pp: 583-588.
- Baba, Y., S. Miyazaki and M. Ishii, 2004. Reproduction of lightning electromagnetic field waveforms by engineering model of return stroke. IEEE Trans. Electromagnet. Compat., 46-1: 130-133.
- Heidler, F., 1985. Analytische biltzstrom-funktion zur LEMP Berechnung. In: Proceeding of the International Conference on Lightning Protection, München, Deutschland, pp: 63-66.
- Nucci, C.A., F. Rachidi, M. Ianoz and C. Mazetti, 1993. Lightning-induced voltages on overhead power lines. IEEE Trans. Electromagnet. Compat., 35-1: 183-189.
- Nucci, C.A., F. Rachidi, M. Ianoz and C. Mazzetti, 1995. Comparison of two coupling models for lightning induced overvoltage calculations, IEEE Transaction on Power Delivery, 10: 330-336.
- Nucci, C.A. and F. Rachidi, 1999. Lightning induced overvoltages. IEEE Transmission and Distribution Conference, Panel Session: Distribution lightning Protection, New Orleans, USA.
- Paolone, M., C.A. Nucci, E. Petrace and F. Rachidi, 2004. Mitigation of lightning induced overvoltages in medium voltage distribution lines by means of periodical grounding of shielding wires and of surge arresters: Modeling and experimental validation. IEEE Transaction on Power Delivery, 19-1: 423-431.
- Rachidi, F., 1991. Effets électromagnétiques de la foudre sur les lignes de transmission aériennes, modélisation et simulation. École Polytechnique Fédérale de Lausanne, Switzerland.
- Rakov, V.A. and M.A. Uman, 1998. Review and evaluation of lightning return stroke models including some aspects of their application. IEEE Trans. Electromagnet. Compat., 40-4: 403-426.

- Rakov, V.A., 2001. Characterization of lightning electromagnetic fields and their modeling. In Proceeding of the 14th International Symposium. On Electromagnetic Compatibility, 20-22 February, Zurich, Switzerland.
- Rubinstein, M. and M.A. Uman, 1989. Methods for calculating the electromagnetic field from a known source distribution: Application to lightning.. IEEE Trans. Electromagnet. Compat., 31-2: 183-189.
- Rubinstein, M. and M.A. Uman, 1991. Transient electric and magnetic fields associated with establishing a finite electrostatic dipole, revisited. IEEE Trans. Electromagnet. Compat., 33-4: 312-320.
- Sadiku, M.N.O., 1992. Numerical Techniques in Electromagnetics. CRC Press, New York
- Sarto, M.S., 2001. Innovative absorbing-boundary conditions for the efficient fdtd analysis of lightning-interaction problems. IEEE Transaction Electromagnet. Compat., 43-3: 368-372.
- Sartori, C.A.F. and J.R. Cardoso, 2000. An analytical-FDTD method for near LEMP calculation. IEEE Trans. Magnet, 36-4: 1631-1634.
- Shoory, A., R. Moini and S.H.H. Sadeghi, 2003. Analysis of lightning electromagnetic fields in the vicinity of a lossy ground, using a new antenna theory model. In Proceeding of IEEE Bologna Power Tech. Conference, June 23-26, Bologna, Italy.
- Tirkas, P.A., C.A. Balanis, M.P. Purchine and G.C. Barber, 1993. Finite-difference time-domain method for electromagnetic radiation, interference and interaction with complex structures. IEEE Trans. Electromagnet. Compat., 35-2: 192-203.
- Uman, M.A. and D.K. McLain, 1971. Exact expression and moment approximation for the electric field intensity of the lightning return stroke. J. Geo. Phys. Res., 76: 2101-2105.
- Yang, C. and B. Zhou, 2004. Calculation methods of electromagnetic fields very close to lightning. IEEE Trans. Electromagnet. Compat., 46-1: 133-141.
- Yee, K.S., 1966. Numerical solution of initial boundary values problems involving Maxwell's equations in isotropic media. IEEE Trans. Antenna Propagation, 14-3: 302-307.